Mass Transfer at Low Flow Rates in a Packed Column

V. P. DORWEILER and R. W. FAHIEN

Iowa State College, Ames, Iowa

Mass transfer in packed columns has been investigated for a variety of column and packing sizes but at flow rates restricted to fully developed turbulent conditions. The present work was undertaken to investigate mass transfer at flow-rate conditions in the transition and laminar regions.

A dual treatment of experimental data required a knowledge of the variation of concentration and velocity with radial position. A tracer-injection technique was employed which consisted in the introduction of a tracer gas into the center of a bulk gas stream and the measurement of the tracer-gas concentration at various radial positions downstream. The velocity distribution for the packed column was determined by means of a five-loop, circular, hot-wire anemometer. The test column was a vertical 4-in. pipe, packed with ¼-in. spherical, ceramic catalyst-support pellets.

Mass transfer diffusivity and Peclet number were determined from two solutions of the differential-diffusion equation applied in previous investigations. An analytical solution in terms of Bessel functions was used to calculate values of average diffusivity and Peclet number and a seminumerical solution in terms of homogeneous linear-difference equations to calculate values of point diffusivity and Peclet number.

Variation of diffusivity and Peclet number with radial position is shown, average diffusivity and Peclet number being correlated with Reynolds number. The interaction of molecular and eddy mass transfer mechanisms with decreasing mass velocity is illustrated by defining a molecular and an eddy Peclet number and correlating with Reynolds number. Eddy diffusivity is correlated as a function of local flow conditions.

This paper presents a continuation of a previous study of mass transfer in a packed system (*1*). In the first paper mass transfer was investigated in the turbulent region for a range of column and packing sizes; the present study considered the flow range over which a separation of molecular and eddy mechanisms could be obtained. Consequently the lower velocity streams in the laminar and transition regions were investigated as well as the initial points of the fully developed turbulent region.

The general expression for the rate of mass transfer is

$$N_A = -\underline{E}\frac{\partial C}{\partial y} \qquad (1)$$

Two previous studies of mass transfer in packed systems differed in the approach used in the definition of diffusivity. Bernard (*2*) considered diffusivity to be independent of position in the system. An average diffusivity was thereby obtained which is an average for all flow conditions throughout the system. The approach used in the previous work (*1*) was to permit diffusivity and velocity to vary with radial position. A "point" diffusivity was obtained which is a function of position in the system, that is of point flow conditions.

These two mathematical techniques, used to solve the basic differential equation for mass transfer under the different assumptions, were employed in this work, to obtain a wider expression for the mass transfer parameters. The average diffusivity was analyzed for molecular and eddy contributions, and the variable term was analyzed for an expression relating diffusivity with point flow conditions and radial position. While the packed column is not a general system for the study of mass transfer, the techniques of definition and calculation derived herein are not restricted to this system.

V. P. Dorweiler is with Standard Oil Company (Indiana), Whiting, Indiana.

EQUIPMENT AND PROCEDURE

The general experimental equipment used in this study was described in detail in the previous paper (*1*). The only new piece of apparatus introduced was a five-loop, circular hot-wire anemometer used to determine the velocity distribution across the packed bed. Figure 1 is a schematic representation of the anemometer. Platinum wire of 0.006-in. diameter was used for the loops. Construction details and calibration procedures are discussed by Schwartz (*3*).

The experimental procedure to obtain concentration data was essentially that described previously. The technique for velocity determination in the packed system (*3*) indicated that an optimum position above the bed exists for the measurement of velocities representing the true distribution in the packing. If the loops are located lower than this optimum position, the extreme turbulence of the gas emerging from the packing (radial velocities of the air emerging from restricted flow and returning to empty tube conditions) would cause the anemometer to indicate too high a velocity owing to the cooling by these radially directed velocity components. If the anemometer were higher, a return of the velocities to an empty-tube distribution would be obtained. The anemometer was operated at 1 in. above the bed in this investigation, after this was determined experimentally as an optimum height.

CALCULATION OF RESULTS

The basic differential equation for mass transfer, which considers diffusion in the radial direction only and bulk flow in the axial direction, is

$$\frac{\partial}{\partial r}\left(\underline{E}r\frac{\partial C}{\partial r}\right) = ur\frac{\partial C}{\partial z} \qquad (2)$$

Angular symmetry is assumed. The following boundary conditions are imposed:

1. At $z = 0$, the plane of the injection tube tip

$$C(r, 0) = C_f, \quad \text{for} \quad 0 < r < t$$

and

$$C(r, 0) = 0, \quad \text{for} \quad t < r < r_0$$

2. At the tube wall

$$\frac{\partial C(r_0, z)}{\partial r} = 0$$

3. At the tube center

$$\frac{\partial C(0, z)}{\partial r} = 0$$

Analytical Solution

On the assumption that $\underline{E}$ and u are independent of position, the solution of Equation (2) presented by Bernard (*2*) and modified by Kurihara (*4*) is in the form of an infinite Fourier-Bessel series

$$\frac{C}{C_A}\frac{C_A}{C_M} = 1 + \frac{2}{t}\sum_{n=1}^{\infty}\frac{1}{\beta_n}\frac{J_1(\beta_n t)}{J_0(\beta_n r_0)} J_0(\beta_n r)\exp\left(-\beta_n^2 z/\alpha\right) \qquad (3)$$

The series converges rapidly for small values of C_{max}/C_{min}; that is z is sufficiently great. The reduced form of Equation (3) is

$$\frac{C}{C_A}\frac{C_A}{C_M} = 1 + \frac{2}{t\beta_1}\frac{J_1(\beta_1 t)}{J_0^2(\beta_1 r_0)} J_0(\beta_1 r)\exp\left(-\beta_1^2 z/\alpha\right) \qquad (4)$$

Concentration at the column center, where $r = 0$, is given by

$$\frac{C_0}{C_A}\frac{C_A}{C_M} = 1 + \frac{2}{t\beta_1}\frac{J_1(\beta_1 t)}{J_0^2(\beta_1 r_0)}\exp\left(-\beta_1^2 z/\alpha\right) \qquad (5)$$

By plotting C/C_A vs. $J_0(\beta_1 r)$ one can obtain the value of C_0/C_A analytically. The intercept of such a linear plot is C_M/C_A. Since all of the other terms of Equation (5) are then known, α can be calculated. The average Peclet number can also be calculated, since

$$Pe = D_p\frac{V}{\underline{E}} = D_p\alpha \qquad (6)$$

Equation (4) was applied in this investigation by the fitting of the experi-

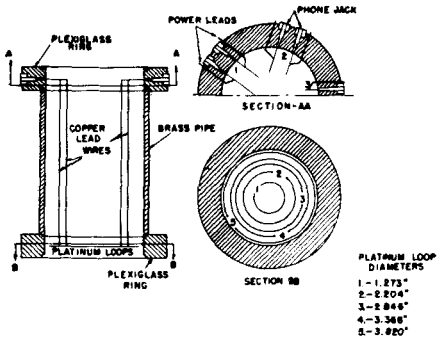

Fig. 1. Hot-wire anemometer.

mental concentration data to a linear relationship with the first-order Bessel function by the least squares procedure. The analytical determination of C_M/C_A differs from that employed by Bernard, which was a graphical integration of point concentration data on an area-weighted basis. The analytical procedure was preferred, since more dependence on the linear relationship is necessarily involved.

Illustration of Analytical Solution

Application of least squares to the experimental concentration data, for a run at a mass velocity of 214 lb./sq. ft./hr., established the following best line:

$$\frac{C}{C_A} = 0.6404\ J_0(\beta_1 r) + 1.086 \qquad (7)$$

The value of $C_M/C_A = 1.086$, and $C_0/C_A = 1.726$. The value of C_0/C_M then is 1.516. From Equation (4)

$$1.516 = 1 + \frac{2}{(0.435/2)(1.904)} \times \frac{J_1(1.904 \times 0.435/2)}{J_0^2(1.904 \times 2.013)} \times \exp(-1.904^2 \times 30.4/\alpha)$$

$$= 1 + 6.003 \exp(-145.459/\alpha)$$

$$= 1 + 6.003 \exp(-28.839/Pe)$$

The α ratio and Peclet number are

$$\alpha = 44.897 \text{ in.}^{-1}, \quad \text{and} \quad Pe = 11.74$$

Diffusivity, in terms of the corresponding flow rates, is given as the reciprocal of the α ratio

$$\underline{E}/V = 0.0223 \text{ in.}$$

Since V is based upon superficial column area, any $\underline{E}$ calculated from this ratio will also be on a superficial basis; the α ratio is however a ratio of the true restricted terms

$$\frac{V/\delta}{\underline{E}/\delta} = \frac{V}{\underline{E}} = \alpha$$

Seminumerical Solution

Under the rigid assumptions that the mass transfer process is a function of local

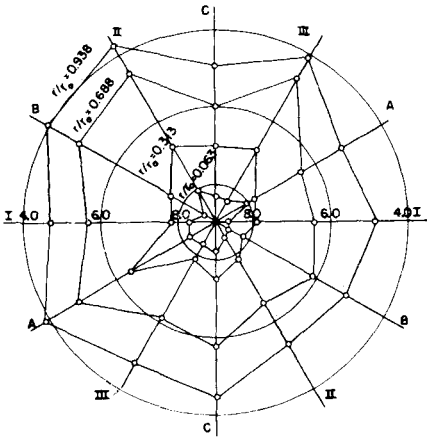

Fig. 2. Variation of concentration with angular position.

flow conditions and that the velocity and diffusivity vary with position in the system, Equation (2) involves functional relations between diffusivity and velocity with radial position. Since the nature of these relations is unknown, an analytical solution is not possible. A seminumerical method was employed in the previous work (*1*) to solve the equation. Equation (2) was replaced by a system of difference equations written about points over the radius. This system is linear in the eigen functions at each interval about the point and in the eigen value. Solution of Equation (2) is of the form

$$C = \sum_{n=0}^{N} A_n R_n \exp(-\lambda_n z/r_0^2) \qquad (8)$$

A simplification in the solution is possible. Since Equation (8) involves negative exponential terms in z and λ, and since λ increases with n, the series converges rapidly for a sufficiently large Z:

$$C = A_0 R_0 Z_0 + A_1 R_1 Z_1 \qquad (9)$$

when one applies boundary conditions 1 to 3 and imposes the orthogonality of the eigen functions, a direct solution for diffusivity is available in the form

$$\underline{E}_{k+1/2} = \frac{\lambda_1 h^2 \sum_{k=0}^{k} P_k(C_k - C_M)}{\theta_{k+1/2}(C_k - C_{k+1})} \qquad (10)$$

The value of λ_1 is given by

$$\lambda_1 = -\frac{r_0^2}{z} \ln Z_1 \qquad (11)$$

where

$$Z_1 = \frac{\sum_{k=0}^{N} P_k(C_k - C_M)^2 \times \sum_{k=0}^{t} P_k}{\sum_{k=0}^{t} P_k(C_k - C_M) \times \sum_{k=0}^{N} C_k P_k} \qquad (12)$$

The mean integral concentration is obtained by a volumetric flow rate-weighted average of point concentrations:

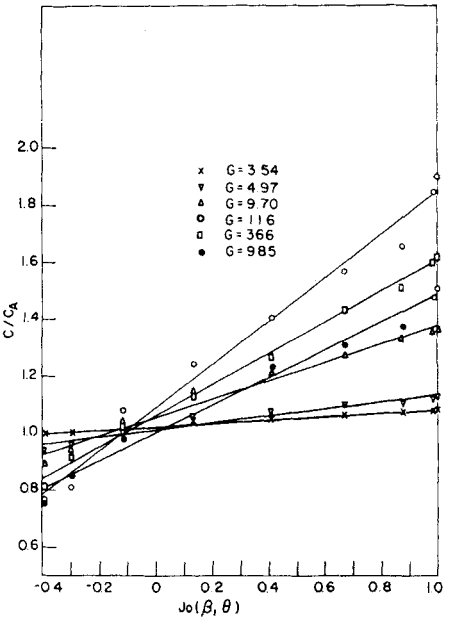

Fig. 3*a*. Variation of concentration with Bessel function of zero order, Equation (11).

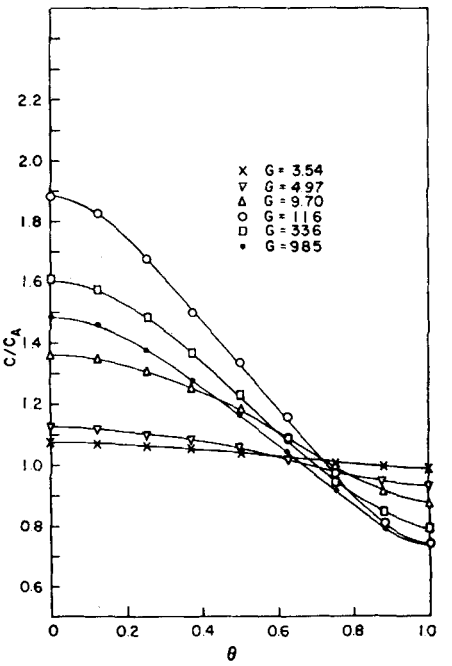

Fig. 3*b*. Variation of concentration with radial position.

$$C_M = \frac{\int_0^1 Cu\theta\, d\theta}{\int_0^1 u\theta\, d\theta} = \frac{\sum_{k=0}^{N} C_k P_k}{\sum_{k=0}^{N} P_k} \qquad (13)$$

Illustration of Seminumerical Solution

The seminumerical solution is illustrated in Table 1, which has been subdivided to illustrate better the details involved.

RESULTS

Concentration data in the form of C/C_A ratios were used directly in the

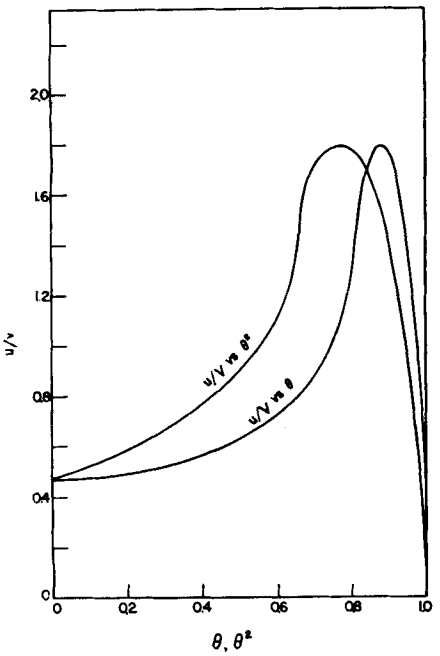

Fig. 4*a*. Variation of velocity with radial position.

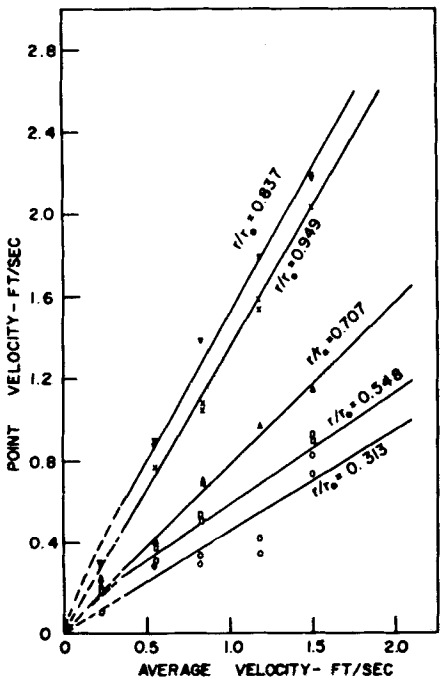

Fig. 4*b*. Variation of velocity profile with mass velocity.

mathematical analysis, since the analytical solution is of this form, and the numerical solution involves a homogeneous ratio of concentrations. Similarly velocity data in the form of u_k/V ratios were used directly in the seminumerical solution to yield values of $E_{k+1/2}/V$ corresponding to the α ratio.

Figure 2 illustrates the deviation of the test bed from perfect angular symmetry of packing, which was assumed in both solutions. The concentration data used represent the average of six points of radial symmetry, thereby weighting the concentrations throughout the bed.

TABLE 1. SEMINUMERICAL SOLUTION

Positions		Calculation of C_M			Calculation of Eigen Value				Calculation of Diffusivity and Peclet Number				
k	θ	C_k/C_A	u_k/V	P_k/V	C_kP_k/V	$\frac{C_k-C_M}{C_A}$	$\frac{P_k}{V}\frac{(C_k-C_M)}{C_A}$	$\frac{P_k}{V}\frac{(C_k-C_M)^2}{C_A^2}$	$\sum\frac{P_k}{V}\frac{(C_k-C_M)}{C_A}$	$\frac{C_k-C_{k+1}}{C_A}$	$\frac{E_k}{V}$(in.)	$\frac{u_k}{V}$	(Pe)k	k
0	0.000 0.063	1.726	- 0.474	0.0074[a]	0.0128	0.752	0.00557	0.00419	0.00557	0.042	0.0115	0.474	10.81	1/2
1	0.125 0.188	1.684	0.480	0.0600	0.1010	0.710	0.04260	0.03025	0.04817	0.114	0.0122	0.491	10.55	1 1/2
2	0.250 0.313	1.570	0.506	0.1265	0.1986	0.596	0.07539	0.04494	0.12357	0.141	0.0152	0.527	9.09	2 1/2
3	0.375 0.438	1.429	0.550	0.2063	0.2947	0.455	0.09384	0.04270	0.21741	0.153	0.0176	0.582	8.68	3 1/2
4	0.500 0.563	1.276	0.624	0.3120	0.3981	0.302	0.09422	0.02846	0.31163	0.162	0.0185	0.679	9.51	4 1/2
5	0.625 0.688	1.114	0.749	0.4681	0.5215	0.140	0.06544	0.00918	0.37717	0.147	0.0202	0.850	11.03	5 1/2
6	0.750 0.813	0.967	1.018	0.7635	0.7383	-0.007	-0.00535	0.00004	0.37183	0.135	0.0183	1.462	20.88	6 1/2
7	0.875 0.938	0.832	1.805 1.548	1.5794	1.3140	-0.142	-0.22427	0.03185	0.14756	0.060	0.0142	1.548	28.58	7 1/2
8	1.000	0.772	-	0.7254[b]	0.5602	-0.202	-0.14658	0.02961	0.00098					
				4.2488	4.1393			0.22119						

$$\frac{C_M}{C_A} = \frac{\sum_0^N C_kP_k}{\sum_0^N P_k} = \frac{4.1393}{4.2488} = 0.974$$

$$\frac{1}{Z_1} = \frac{\sum_0^N C_kP_k/C_A}{\sum_0^N P_k(C_k-C_M)^2/C_A^2} \times \frac{\sum_0^{c_t} P_k(C_k-C_M)/C_A}{\sum_0^t P_k} = \frac{4.1393}{0.2212} \times \frac{(0.00557 + \frac{0.1152}{0.1250}\,0.04260)}{(0.0074 + \frac{0.1152}{0.1250}\,0.0600} = 13.381$$

$$\lambda_1 = \frac{r_0^2}{2} \ln\left(\frac{1}{Z_1}\right) = \frac{2.013^2}{30.4} \ln 13.381 = 0.3458 \text{ in}$$

$$\frac{r}{r_0}_{1/2} = \frac{\lambda_1 h^2 \sum_{k=0}^{\frac{1}{2}} \frac{P_k}{V}(C_k-C_M)}{\theta_{3\,1/2}\,(C_3-C_4)} = \frac{(0.3458)\,(1/8)^2(0.2174)}{(0.438)\,(0.153)} = 0.0176 \text{ in.} \qquad (Pe)_{3\,1/2} = \frac{D_p(u_{3\,1/2}/V)}{(E_{3\,1/2}/V)} = \frac{(0.262 \text{ in})(0.582)}{(0.0176 \text{ in})} = 8.68.$$

[a] P_0 is obtained by consideration of an increment of one-half normal width, and must then be equivalent to $1/2P(h/4)$, where $P(h/4)$ is the mean value of P in the region $0 < \theta/2 < h/2$. Since velocity changes negligibly in this region, $P(h/4) = 1/2P(h/2)$, and $P_0 = 1/4P(h/2)$.

[b] By similar reasoning, $P_8 = (1/2)P(7\ 1/2)h\_7$.

[c] Since t is non-integral in k, the summation is performed to the next integral value above t, and the resulting value linearly proportioned. In this application t = 0.1152, which is less than one increment; hence, the t/h fraction is used to proportion the $P_1(C_1-C_M)/C_A$ term.

Figures 3*a*, *b* illustrate the fit of concentration data to the theoretical relations developed in the mathematical solutions. Figure 3*a* represents a plot of Equation (4). The data are seen to scatter seriously at high values of C_0/C_A corresponding to peak values of Peclet number. The linear relationships shown were established by least squares. Figure 3*b* represents a plot of Equation (8). These data are smoothed values fitted to the boundary conditions and used in the seminumerical solution. Scatter of data about the smoothed curves was generally much less than that experienced in the linear fitting.

Velocity distribution across the test bed is shown in Figure 4*a*. This distribution was found to be essentially independent of total flow rate above an average superficial velocity of 0.4 ft./sec., in agreement with the results of Schwartz (*3*). The plot of point velocity vs. average velocity at constant radial position (Figure 4*b*) indicates this independence, as well as the deviation from a uniform distribution at low flow rates. Generally the hot-wire anemometer was found to give a sufficiently accurate material balance only at average velocities above 0.2 ft./sec., which prevents the numerical treatment of data below this velocity.

Average diffusivity and Peclet number, determined over a range of mass velocities from 985 to 3.54 lb./(sq. ft.)(hr.), are shown in Figures 5*a*, *b*, plotted against Reynolds number. The values of average diffusivity and Peclet number are tabulated in Table 2.*

Point diffusivity and Peclet number are shown as functions of radial position in Figures 6*a* and *b*. Point diffusivity was found to be constant at the bed center, to reach a maximum near the column wall, and to decrease at the wall. Point Peclet number was found to be constant at the bed center and to increase as the column wall was approached. An expected decrease of Peclet number at the wall was not detected, since the numerical method yielded an average value at one-half increment away from the wall. Point diffusivity and Peclet number are listed in Tables 3* and 4* for eight mass velocities ranging from 985 to 50.2 lb./(sq. ft.)(hr.)

DISCUSSION OF RESULTS

The scope of this investigation was chosen to cover an extended range of a Peclet number-Reynolds curve, which includes the initial points of a fully developed turbulent region, the full transition region, and the onset of the laminar region. Of special interest was a study of the interaction of eddy and

*Tables 2, 3 and 4 are on file with the American Documentation Institute, Auxiliary Publications Photoduplication Service Library of Congress, Washington 25, D. C., and may be ordered as document No. 5871 on remission of $1.25 for microfilm or $1.25 for photoprints.

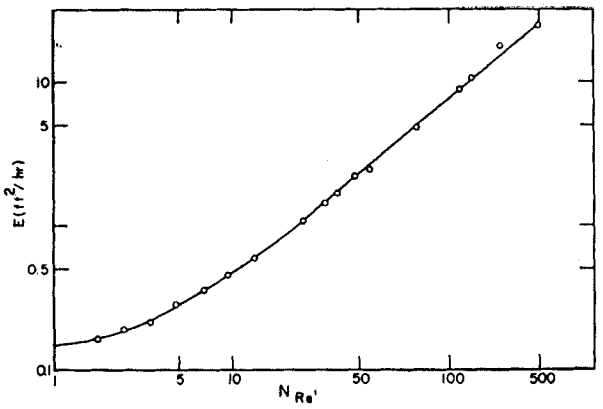

Fig. 5a. Average diffusivity calculated by the analytical method.

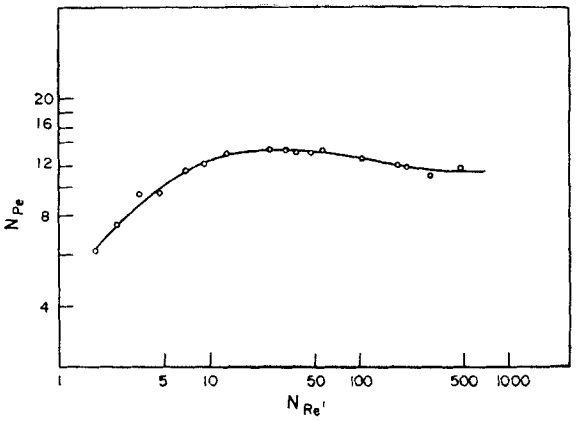

Fig. 5b. Average Peclet number calculated by the analytical method.

molecular mechanisms as the importance of molecular transfer developed.

An inspection of Figure 5b will reveal qualitatively the interaction of eddy and molecular mechanisms. At a Reynolds number above 200 the Peclet number is found to be essentially constant with velocity, as has been demonstrated by Towle and Sherwood (5) and Bernard (2) for empty tubes and in the previous work (1) for packed beds. At a Reynolds number of 200 a break in the curve is observed, corresponding to the departure of eddy diffusivity from a linear relationship with velocity. As Reynolds number (velocity) decreases, the eddy diffusivity decreases more rapidly, with a corresponding increase in Peclet number. With further decrease in Reynolds number the turbulent effects in the bed diminish. Molecular diffusivity, which is independent of velocity, becomes increasingly important, that is of the same order of magnitude as the eddy diffusivity. With further decrease in Reynolds number Peclet number reaches a maximum and then decreases as the eddy diffusivity damps out, ultimately reaching a linear relationship with velocity during completely laminar flow. In Figure 5a diffusivity is seen to assume a limiting value at low Reynolds number. This is presumably the molecular diffusivity. Since this value is determined on a superficial basis, $\alpha = (V/\delta)/D_v$, the limiting value obtained is $D_v\delta$. When one uses a value of $\delta = 0.32$ (6), the value of D_v obtained is 0.45 sq. ft./hr., which agrees with the published value of molecular diffusivity for carbon dioxide in air (7).

An over-all correlation of data from this investigation with those reported from other works is presented in Figure 7. An empirical relation developed previously (1) was used to correlate various column and packing sizes.

THEORETICAL CONSIDERATIONS

A quantitative explanation of mass transfer in a given system is inherently based upon a knowledge of flow conditions existing within the system. Limitations in the precise definition of the nature of these flow conditions impose severe limitations upon an analogous definition of the mechanism of mass transfer. Virtually all previous studies of the diffusional mechanism have concerned themselves with the consideration of fully developed turbulent systems. In general, application of existing theories of turbulence has aided substantially in the understanding of diffusion in these turbulent systems. Application of the theories of turbulence to a system so complex as a packed bed however must be greatly restricted, since many of the basic physical conditions of empty-tube turbulence do not pertain. While in empty tubes eddy displacements are random in length and subjected generally only to tube-wall restrictions, in packed beds these are controlled by randomly arranged interstitial channels. While the scale of turbulence decreases, the intensity of turbulence is seen to increase. Still further complexities are introduced by the coexistence of laminar and turbulent conditions within individual voids.

The mass transfer mechanism in a packed bed has been described on a theoretical basis with a completely developed state of turbulence (complete mixing within a void and sufficiently high velocities with a correspondingly large number of fluid elements into and out of a void) for a regular packing arrangement assumed. In accordance with the random walk theory (8) Peclet number is given by

$$N_{Pe} = c\,\frac{1 - R_x}{1 + R_x} \qquad (14)$$

with $R_x = -1$ indicating laminar conditions and $R_x = 0$ indicating complete mixing. The increase in Peclet number with radial position can be explained on a semitheoretical basis as a result of a change in the correlation coefficient from a value near zero throughout the center portion of the bed to negative values nearer the wall, with $R_x = -1$ giving an infinite Peclet number. This is a semitheoretical approach, since the derivation of the random walk theory depends upon the existence of complete

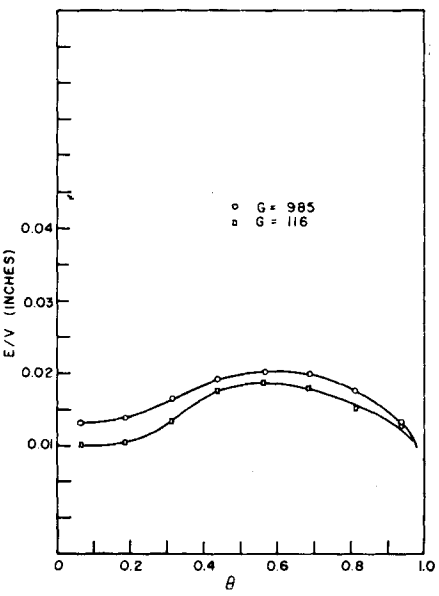

Fig. 6a. Variation of diffusivity with radial position.

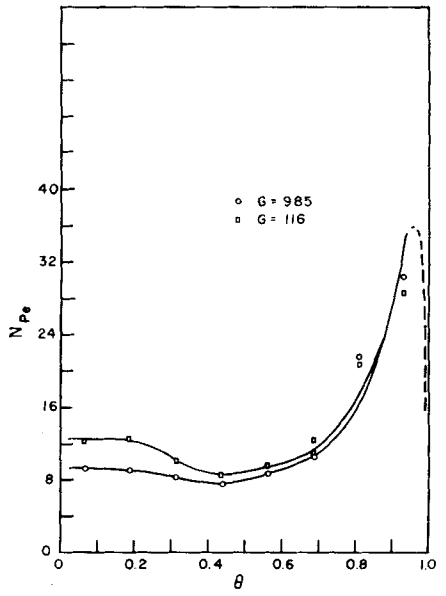

Fig. 6b. Variation of Peclet number with radial position.

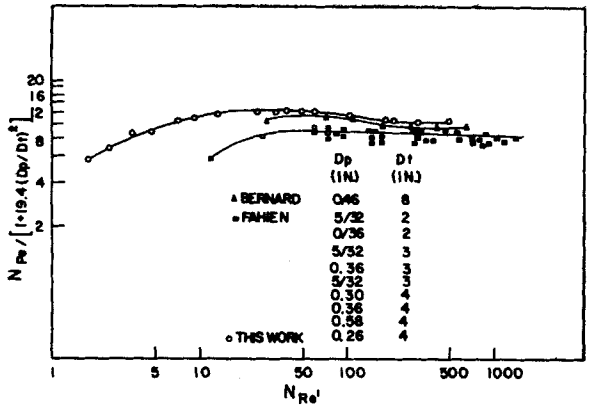

Fig. 7. Correlation of average Peclet number with Reynolds number and D_p/D_t .

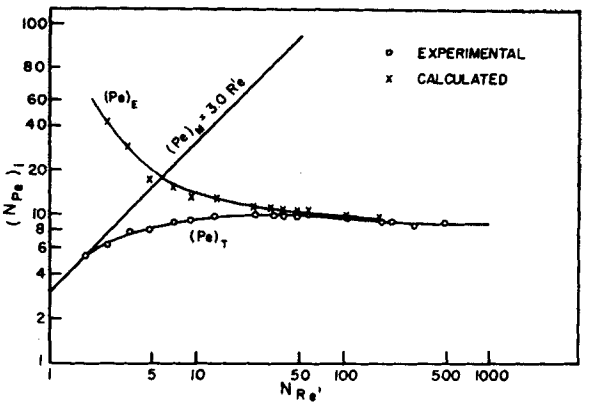

Fig. 8. Correlation of molecular, eddy, and total Peclet numbers with modified Reynolds number.

turbulence, that is, the correlation coefficient being constant at zero.

Bernard (*2*) used pressure-drop data to determine the nature of turbulence in a packed bed. Since experimental friction-factor–Reynolds-number curves indicated no sharp breaks over the transition region (defined by the break in Peclet-number–Reynolds-number curve) as contrasted with the discontinuity in the empty tube curve, the turbulence existing within the bed is seen to develop gradually over the range of flows. The correlation of pressure-drop and mass transfer data with the packing diameter used as the length parameter seems to indicate that interstitial turbulence is a function of packing sizes.

The continuous nature of the friction-factor–Reynolds-number curves does not indicate the physical significance of the transition point in Peclet-number–Reynolds-number curves. This was postulated by Bernard from the following experimental observations. In liquid systems large eddies with scales up to several particle diameters were observed for flow rates considerably below turbulent values. The pressure drop, which is essentially dependent on flow conditions in the interstices between packing particles, would therefore not reflect the existence of these large eddies, and in turn these large eddies cannot be assumed to cause the interstitial turbulence. When one considers that the Reynolds number point of departure of the transition region from the turbulent region was found to increase in magnitude directly with D_p/D_t or to remain fixed with a Reynolds number based upon D_t, the transition region is thought to be created by these large eddies, which apparently are generated under conditions similar to empty-tube conditions. Further at fully developed turbulent conditions the large eddies were no longer present.

These two systems, while in agreement from pressure-drop considerations, are irresolvable in an attempt to define a mass transfer mechanism on the basis of either. Point diffusivity was found to be proportional to both factors, that is proportional to column diameter near the wall and to pellet diameter near the bed center. Any development of a diffusional mechanism must then consider both processes. Yet any attempt to visualize a mechanism for mass transfer is generally reduced to a consideration of a single void. Perhaps then the most significant approach is to analyze an over-all mechanism, as is suggested by the average data obtained from the analytical solution, and also to analyze a variable mechanism, as is suggested by point data obtained from the numerical solution.

Average Diffusivity Data

Since the molecular and the eddy mechanisms are seen to be involved in the over-all process, a parallel transfer is perceivable:

$$\underline{E} = D_v + E \qquad (15)$$

or when one rearranges

$$\frac{1}{1/\underline{E}} = \frac{1}{1/D_v} + \frac{1}{1/E} \qquad (16)$$

and when one divides through by $D_v V$,

$$\frac{1}{(N_{Pe})_T} = \frac{1}{(N_{Pe})_M} + \frac{1}{(N_{Pe})_E} \qquad (17)$$

A means of determining the molecular term is now found in the Peclet number defining identity

$$(N_{Pe})_M = N_{Re''}(N_{Sc})_M \qquad (18)$$

where

$$N_{Re''} = D_p \frac{\rho(V/\delta)}{\mu} \qquad (19)$$

and

$$(N_{Sc})_M = \frac{\mu}{D_v \rho} \qquad (20)$$

Molecular Peclet number is then given by

$$(N_{Pe})_M = D_p V / D_v \delta \qquad (21)$$

When a void fraction of 0.32 (*6*), with a value of unity for the molecular Schmidt

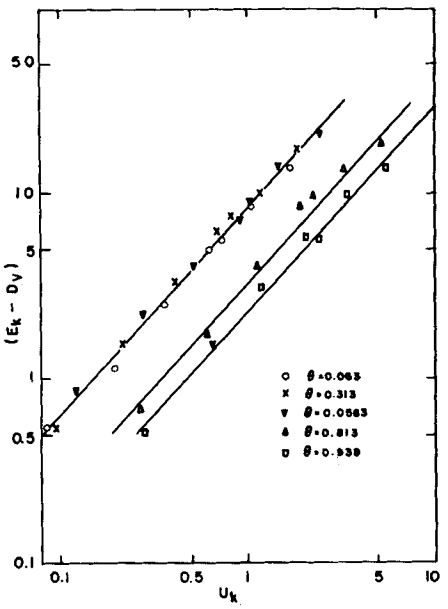

Fig. 9*a*. Velocity function, Equation (31).

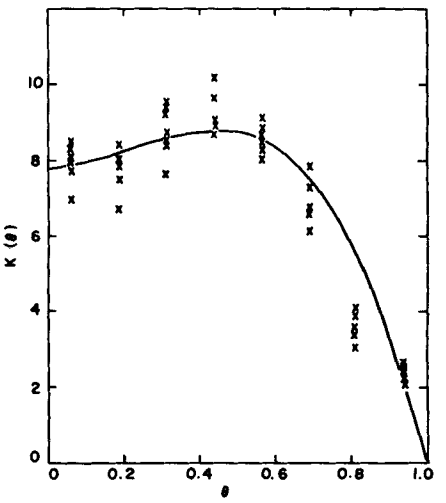

Fig. 9*b*. Position function, Equation (32).

number, is assumed, the molecular Peclet number is

$$(N_{Pe})_M = 3.13N_{Re'} \qquad (22)$$

The eddy Peclet number can then be calculated from Equation (17).

The average Peclet numbers were treated in this manner. The resulting values of eddy and molecular Peclet numbers as well as the total Peclet number are plotted against Reynolds number in Figure 8. Eddy Peclet number is seen to be indistinguishable from total Peclet number for Reynolds numbers above 300, to increase quite gradually from this identity with total Peclet number for Reynolds number between 300 and 30, and to increase sharply at a Reynolds number of about 8. This last point is interpreted as the point of severe damping of turbulence within the bed.

An inspection of Figure 8 reveals that, consistent with the observations of Bernard, an eddy effect is permissible in this gaseous system down to very low values of Reynolds number. Further as Reynolds number tends toward zero, the eddy mechanism is seen to damp out rapidly, thereby allowing an establishment of completely laminar conditions. The lowest measured effective Peclet number was found to be equal to the theoretical molecular Peclet number, which leads to the conclusion that completely laminar conditions were found to exist.

Point Diffusivity Data

A second approach to the examination of the mass transfer process involves diffusivity as a function of local flow conditions. The nature of this function can then be determined by the fitting of experimental point data to the proposed expression. From Equation (15) the total diffusivity can be expressed as a molecular term and an eddy term, the former being invariant in the system. Hence

$$\underline{E} = D_v + Kf(u, \theta) \qquad (23)$$

The value assumed for the molecular diffusivity in this system was the limiting value of diffusivity shown in Figure 5*a*. By plotting $\underline{E}_k$, or $(E - D_v)_k$, vs. u_k at constant radial positions, one obtains the relationship

$$(\underline{E} - D_v) = K_k u_k^{1.12} \qquad (24)$$

By plotting K_k vs. θ one gets

$$K_k = 7.80(1 + \theta^{1.7} - 2\theta^{3.4}) \qquad (25)$$

Equation (23) then becomes

$$\underline{E}_k = D_v + 7.80u_k^{1.12}(1 + \theta^{1.7} - 2\theta^{3.4}) \qquad (26)$$

Figures 9*a*, *b* show the fit of experimental data to the velocity and position functions.

Equation (26) represents the data for the system investigated in this work. The equation is restricted to the system studied, since no general variation of column or packing size was considered, that is the D_p/D_t parameter. However the general technique of determining velocity and position functions on an empirical basis seems to be a sound approach. Equation (26) can be used to predict diffusivity for the system from a knowledge of the velocity distribution.

The variation of eddy diffusivity with radial position can be interpreted theoretically on the basis of the Prandtl mixing-length definition of diffusivity as the product of deviating velocity and eddy mixing length. Since point velocity and void space, characterizing the deviating velocity and mixing length, both increase near the wall, the diffusivity increases. Near the wall velocity decreases rapidly to zero, while void space increases to unity. The preponderant effect of diminishing velocity decreases diffusivity. Figure 9*b* however illustrates the residual dependence of diffusivity on void space, since the velocity effect has been isolated from the defining function.

CONCLUSIONS

Mass transfer in packed beds can be described as consisting of parallel- and eddy-transfer mechanisms. The molecular contribution is invariant with the physical system and is the sole mechanism operating at very low Reynolds number. The eddy contribution, considered on a point basis, is found to vary with local flow conditions and can be defined on the basis of these flow conditions. From empirical relations eddy diffusivity can be predicted in terms of point velocity, an easily measured operating variable.

The variation of eddy diffusivity can be explained on the basis of velocity and void space variation within the system.

ACKNOWLEDGMENT

This paper is based on a master of science thesis by V. P. Dorweiler, presented to Iowa State College in December, 1956. Work was performed in the Ames Laboratory of the U. S. Atomic Energy Commission.

The authors wish to express their appreciation to the Ames Laboratory of the Atomic Energy Commission for the support of this project.

NOTATION

A = constant in series solution, area
C = concentration, volume % carbon dioxide in air
C_A = measured average concentration
C_f = concentration of pure carbon dioxide in injection tube
C_M = integral average concentration
C_0 = concentration at column center
D_p = pellet diameter, in.
D_t = tube diameter, in.
D_v = molecular diffusivity, sq. ft./hr.
E = eddy diffusivity, sq. ft./hr.
$\underline{E}$ = total effective diffusivity, sq. ft./hr.
G = mass velocity, lb./sq. ft./hr.
h = interval size in numerical solution
J_0 = zero-order Bessel function of first kind
J_1 = first-order Bessel function of first kind
k = number of position of radial point
K = position function of eddy diffusivity
K_k = constant for given radial position
n = index of summation
N = total number of intervals in numerical solution
N_{Pe} = Peclet number, $D_pV/\underline{E}$
$N_{Re'}$ = modified Reynolds number, D_pG/μ
$(N_{Sc})_M$ = Schmidt number, $\mu/\rho D_v/D_M$
P_k = weight function in numerical solution = $u_k\theta_k$
r = radial distance from center of bed, with r_0 the tube radius, in.
R = eigen function representing the radial variation of concentration
R_x = correlation coefficient
t = radius of injector tube, in.
u = superficial point velocity, ft./sec.
V = superficial average velocity, ft./sec.
z = height of packed bed above injector tube, in.
Z = function representing the axial variation of concentration

Greek Letters

α = ratio of V/E, ft.$^{-1}$
$\beta_n r_0$ = roots of $J_1(\beta_n r_0) = 0$
δ = void fraction
λ = eigen constant in numerical solution
ρ = density, lb./cu. ft.
θ = dimensionless radial position term, r/r_0
μ = absolute viscosity, lb. mass/ft./sec.

LITERATURE CITED

1. Fahien, Raymond W. and J. M. Smith, *A.I.Ch.E. Journal*, **1**, 28 (1955).
2. Bernard, R. A., and R. H. Wilhelm, *Chem. Eng. Progr.*, **46**, 233 (1950).
3. Schwartz, Clarence E., and J. M. Smith, *Ind. Eng. Chem.*, **45**, 1209 (1953).
4. Kurihara, Hiroo M., M.S. thesis, Purdue Univ., Lafayette, Indiana (1954).
5. Towle, W. L., and T. K. Sherwood, *Ind. Eng. Chem.*, **31**, 457 (1939).
6. Schaffer, Michael R., M.S. thesis, Purdue Univ., Lafayette, Indiana (1952).
7. Sherwood, T. K., and R. L. Pigford, "Absorption and Extraction," McGraw-Hill, New York (1952).
8. Latinen, George A., Ph.D. thesis, Princeton Univ., Princeton, New Jersey (1954).

Manuscript received January 7, 1958; revision received August 4, 1958; paper accepted August 6, 1958.